Abstract: Slope stability analysis is one of the oldest geotechnical engineering subjects, yet as we enter the 21st century it remains one of the most active areas of study for geotechnical practitioners and researchers. The 26 state-of-the-art papers contained within this publication entitled *Slope Stability 2000* cover many facets of the subject, including case histories of both natural and constructed slopes, slope stabilization methods, rock slope analysis, shear strength evaluation, centrifuge testing, limit analysis, 3-D analyses, finite element and finite difference methods, progressive failure analyses, and probabilistic methods using Bayesian and random field approaches. It is hoped that readers of *Slope Stability 2000* will be stimulated and inspired by this wide range of quality papers written by a distinguished group of national and international authors.

Library of Congress Cataloging-in-Publication Data

Geo-Denver 2000 (2000 : Denver, Colo.)
Slope stability 2000 : proceedings of sessions of Geo-Denver 2000 : August 5-8, 2000, Denver, Colorado / sponsored by the Geo-Institute of the American Society of Civil Engineers ; edited by D.V. Griffiths, Gordon A. Fenton, Timothy R. Martin.
p. cm. (Geotechnical special publication ; no. 101)
Includes bibliographical references and index.
ISBN 0-7844-0512-3
1. Slopes (Soil mechanics)—Congresses. 2. Soil stabilization—Congresses. 3. Engineering geology—Mathematical models—Congresses. I. Griffiths, D. V. II. Fenton, Gordon A. III. Martin, Timothy R. VI. American Society of Civil Engineers. Geo-Institute. V. Title. VI. Series.

TA710.A1 G34 2000a
624.1'51363--dc21 00-042139

Library of Congress Catalog Card No: 00-042139 ISBN 0-7844-0512-3
Manufactured in the United States of America.

GEOTECHNICAL SPECIAL PUBLICATION NO. 101

SLOPE STABILITY 2000

PROCEEDINGS OF SESSIONS OF GEO-DENVER 2000

SPONSORED BY
The Geo-Institute of the American Society of Civil Engineers

August 5-8, 2000
Denver, Colorado

EDITED BY
D.V. Griffiths
Gordon A. Fenton
Timothy R. Martin

GEO INSTITUTE

ASCE American Society of Civil Engineers
1801 ALEXANDER BELL DRIVE
RESTON, VIRGINIA 20191–4400

Importance of Three-Dimensional Slope Stability Analyses in Practice

David Arellano[1], Student Member and Timothy D. Stark[2], Associate Member

Abstract

This paper focuses on the importance of three-dimensional (3D) slope stability analyses in practice. Commercially available 3D slope stability software does not consider the shear resistance along the two sides of the slide mass that parallel the direction of movement in calculating the 3D factor of safety (Stark and Eid 1998). Consequently, the 3D factor of safety may be underestimated and the back-calculated shear strengths may be overestimated or unconservative. A method for incorporating the shear resistance along the two sides of a slide mass in existing 3D software is presented. A parametric study is used to investigate the importance of 3D end effects by providing a comparison of two-dimensional (2D) and 3D analyses for various slide mass geometries and shear strengths along the failure surface. A field case history is used to illustrate the use of the parametric study results and the importance of conducting a 3D analysis in practice.

Introduction

Two-dimensional (2D) limit equilibrium methods are based on a plane-strain condition. It is assumed that the failure surface is infinitely wide such that three-dimensional (3D) effects are negligible compared to the overall driving and resisting forces. A 2D analysis yields a conservative estimate of the factor of safety because the shear resistance along the two sides of the slide mass or end effects are not included in the 2D estimate of the factor of safety. In general, a 2D analysis is

----

[1]Graduate Research Assistant, Dept. of Civ. and Env. Eng., Univ. of Illinois, 205 N. Mathews Ave., Urbana, IL 61801-2352.

[2]Prof. of Civ. and Env. Eng., Univ. of Illinois, 205 N. Mathews Ave., Urbana, IL 61801-2352.

appropriate for slope design because it yields a conservative estimate of the factor of safety (Duncan 1992). A 3D analysis is recommended for back-analysis of slope failures so the back-calculated shear strength reflects the 3D end effects (Stark and Eid 1998). The back-calculated shear strength then can be used in remedial measures for failed slopes or slope design at sites with similar conditions. If the 3D end effects are not included, the back-calculated shear strengths may be too high or unconservative. A 3D analysis may also be useful to analyze slopes with a complicated topography, large differences in shear strength between the foundation materials and/or overlying materials, and/or a complex pore-water pressure condition because a 3D analysis can incorporate the spatial variation of each of these effects in the calculation of the 3D factor of safety.

Commercially available 3D slope stability software does not consider the shear resistance along the two sides of a slide mass that parallel the direction of movement in calculating the 3D factor of safety (Stark and Eid 1998). Some of the software can incorporate the shear resistance along inclined sides of a slide mass, such as the scarp, but not along vertical sides such as the flanks or parallel sides of the slide mass. As a result a method for incorporating the shear resistance along the vertical sides of a slide mass is presented herein. A parametric study investigates the importance of incorporating 3D effects by providing a comparison of 2D and 3D analyses for various geometries and shear strength conditions. The objective of performing this parametric study was to present the results of 2D and 3D slope stability analyses in a manner that can be used by engineers to determine if a 3D slope stability analysis should be conducted for a particular situation. A field case history is used to illustrate the use of the parametric study results and the importance of conducting a 3D analysis in practice.

Parametric Slope Model

A translational failure mode was selected for use in the parametric study for the following reasons (Stark and Eid 1998): (1) Slopes failing in translational mode usually involve either a significantly higher or lower mobilized shear strength along the back scarp and sides of the slide mass than that along the base, e.g., the upstream slope failure in Waco dam (Beene 1967; Wright and Duncan 1972) and the slope failure in Kettleman Hills hazardous waste repository (Seed et al 1990; Byrne et al. 1992; and Stark and Poeppel 1994), respectively. These situations can result in a significant difference between the 2D and 3D factors of safety. This difference is less pronounced in slopes failing in rotational mode because they usually involve homogenous materials. (2) A translational failure can occur in relatively flat slopes because of the weak nature of the underlying material(s). The flatter the slope, the greater the difference between 2D and 3D factors of safety (Chen and Chameau 1983; Leshchinsky et al. 1985). (3) A translational failure often involves a long and nearly horizontal sliding plane through a weak soil layer [e.g., Maymont slide (Krahn et al. 1979), Gardiner Dam movement (Jasper and

Peters 1979), and Portuguese Bend slide (Ehlig 1992)] or geosynthetic interface, e.g., Kettleman Hills repository. The presence of a well-defined weak layer or interface provides some certainty in the shear strength input data. (4) A translational failure often involves a drained shearing condition. This facilitates estimation of the mobilized shear strength of the materials involved because shear-induced pore-water pressures do not have to be estimated.

Figs. 1 and 2 show the 3D geometry for the slope model used in the parametric study. Three slope inclinations, 1H:1V, 3H:1V, 5H:1V, were investigated. For each slope inclination, heights of 10 and 100 m were analyzed. For the slope height (H) of 10 and 100 m, width (W) to height ratios (W/H) of 1, 1.5, 2, 4, 6, 8, and 10 were analyzed. Thus, for a slope height of 10 m, slope widths of 10, 15, 20, 40, 60, 80, and 100 m were analyzed and for an H of 100 m, widths of 100, 150, 200, 400, 600, 800, and 1,000 m were analyzed. The slope length, L, is dependent on the slope inclination and slope height. The calculated slope lengths resulted in length to height ratios (L/H) of 1.03, 3.30, and 5.88 for slope inclinations of 1H:1V, 3H:1V, 5H:1V, respectively, for both slope heights of 10 and 100 m.

The sides parallel to the direction of movement, not the scarp, of the slide mass in the slope model were assumed to be vertical because the effective normal stress that acts on a vertical surface is only related to the lateral earth pressure and a vertical surface yields the minimum shear surface area. Therefore, in translational failures, vertical sides provide the minimum amount of 3D-shear resistance or end effect.

It can be seen that the slope model in Fig. 2(a) is essentially a rectangle. Of course, actual slide masses are more rounded at the head of the slide mass as well as having other rounded or curved areas. A rounded slide mass was not used because of the difficulties in varying slope length, width, and height with curved ends of the slide mass and obtaining consistent ratios of W/H and L/H. In summary, a rectangular slide mass was used to facilitate the parametric study and provide an insight to the importance of 3D stability analyses in practice.

Two materials, upper and lower, were incorporated in the parametric study as indicated in Fig. 2(b). The lower material was assumed to slope at 3 percent in the direction of sliding to simulate a natural bedding plane or landfill liner system. The saturated unit weights of the upper and lower materials were assumed to be 17 and 18 kN/m^3, respectively. Linear shear strength envelopes passing through the origin with friction angles of 30° and 8° were initially assumed for the upper and lower materials, respectively. The ratio of the friction angle for the upper and lower materials is varied subsequently to investigate the importance of the shear strength difference on the 3D factor of safety.

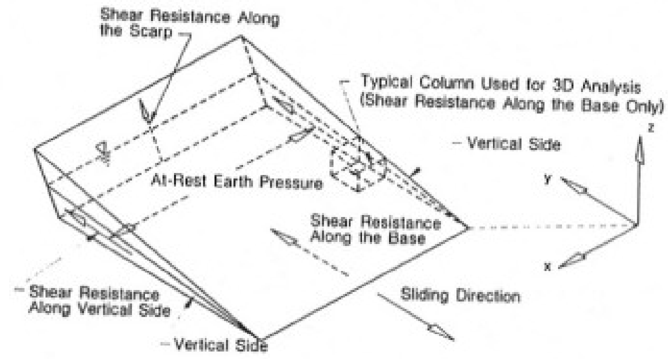

Figure 1. 3D View of Slope Model

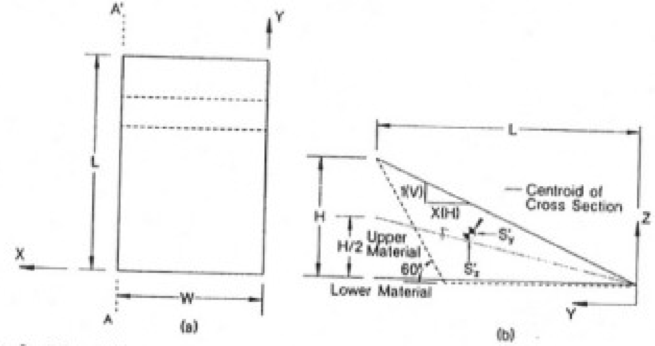

Figure 2. Plan View and Representative Cross Section for Slope Model: (a) Plan View; (b) Cross Section A-A'

In the parametric model, the groundwater level was placed at a height of H/2 as measured at a distance of L from the toe and linearly decreasing to a height of zero at the toe. The scarp was assumed to be inclined at 45° + $\phi_{up}/2$ from the horizontal to simulate an active earth pressure condition where ϕ_{up} is the friction angle of the upper material. This inclination results in a minimum lateral earth pressure condition and a minimum shear resistance along the back scarp during failure. Based on a ϕ_{up} = 30°, the back scarp of the slope model was initially assumed to be inclined at 60° from the horizontal. The bottom of the failure surface extends 0.2 m into the lower material and parallels the upper surface of the lower material until it daylights at the slope toe. The 0.2 m depth was randomly selected to ensure that the slope stability software modeled a translational failure mode with the base of the failure surface within the weak lower layer.

3D Slope Stability Software

In a study to investigate the performance of commercially available 3D slope stability software, Stark and Eid (1998) conclude that CLARA 2.31 (Hungr 1988) facilitated the input process for the slope geometry and pore-water pressure conditions, utilizes Janbu's (1954) simplified method for 2D and 3D analysis which is suitable for a translational failure mode, and can accommodate externally applied loads which can be used to simulate the resistance acting on the vertical sides. As a result, the microcomputer program CLARA 2.31 was used for the parametric study described herein due to the limitations of other 3D software and its capability of performing a 2D analysis from a 3D data file.

Specific information on CLARA 2.31 can be obtained from Hungr (1988, 1989). However, program options utilized for this study are discussed herein. CLARA 2.31 divides the slide mass into vertical columns that are the 3D equivalent of the vertical slices used in a conventional 2D analysis. Geometry data, which is input into CLARA 2.31 through a series of 2D cross sections, for vertical columns between the input 2D cross sections are generated by orthogonal interpolation in this study. The percentage of available array memory, which was used to automatically set the column length and width, used for this parametric study was set at 85 percent for all of the various slope model runs to provide uniform precision between the analyses. The Janbu's simplified method was utilized for this study because the method is suitable for a translational failure mode. The factor of safety obtained from Janbu's simplified method is based on horizontal and vertical force equilibrium. Moment equilibrium is not satisfied. Janbu's simplified method assumes that the resultant intercolumn forces are horizontal and an empirical correction factor is used to account for the interslice vertical force (Janbu 1954). The factor of safety provided by CLARA 2.31 does not include the Janbu correction factor extended to 3D for the effect of the intercolumn force distribution and the results were not adjusted manually to account for this correction.

Stark and Eid (1998) determined that commercially available software does not consider the shear resistance along the parallel sides of a slide mass in calculating the 3D factor of safety. To include this side resistance, an external horizontal and vertical side force equivalent to the shear resistance due to the at-rest earth pressure acting on the vertical sides was added at the centroid of the two parallel sides (see Fig. 2 (b)). From Fig. 3, the at-rest earth pressure acting on the vertical side of the slide mass, σ'_x, is estimated by multiplying the coefficient of earth pressure at rest, K_o, by the average vertical effective stress over the depth of the sliding mass, σ'_z. The coefficient of earth pressure at rest is determined from $K_o = 1\text{-}\sin\phi'_{up}$ where ϕ'_{up} is the friction angle of the upper material corresponding to the average effective normal stress on the vertical sides of the slide mass. The shear resistance due to the at-rest earth pressure acting on the vertical sides of the slide mass, S', is estimated by multiplying σ'_x by the tangent of ϕ_{up}'. In determining S', the shear resistance due to the small thickness and area of lower material between the upper material and the base of the failure surface was not included to simplify the determination of the cross section centroid (see Fig. 2 (b)). Therefore, only the side resistance of the upper layer was included. Additionally, it was assumed that S' acted parallel to the base of the failure surface, at a slope of 3 percent down slope.

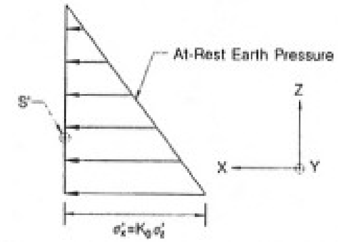

Figure 3. Shear Resistance, S', Due to the At-Rest Earth Pressure Acting on the Vertical Side of the Slope model

External loads are specified in CLARA 2.31 by its horizontal component (S_y') and vertical component (S_z') as depicted in Fig. 2(b) and by its point of application, X, Y, and Z coordinates. The vertical component of an external load is added to the total weight of the column directly below the vertical force if the vertical force is located within the plan area of the slide mass but is not included in the column total weight if the vertical force is located outside of the sliding mass plan area. The external forces applied to the parallel sides of the slide mass are considered to be within the sliding mass plan area. The horizontal component of external loads are included in the horizontal force equilibrium equation, whether or not the point of application is within or outside the plan area of the slide mass.

A 2D analysis was also performed for each geometry using CLARA 2.31 to provide a direct comparison with the 3D factor of safety. Since the slope model used in this parametric study is not rounded at the head scarp, it exhibits uniform cross sections across the slope that yield the same 2D factor of safety. When performing a 2D analysis using CLARA 2.31 from a 3D input file, CLARA 2.31 extracts the 2D cross section of interest from the mesh cross section nearest to the desired section. CLARA 2.31 reverts to a 2D problem by suppressing all input parameters in the third dimension and making all lateral column widths a value of unity. No external loads are utilized in the 2D analyses. It should be noted that the factor of safety obtained from a 3D analysis performed without considering the shearing resistance along the vertical sides of the slide mass (without external loads) yields a similar factor of safety as the corresponding 2D analysis. This confirms that the slope stability program does not consider the shear resistance along the parallel sides of a slide mass in calculating the 3D factor of safety.

Effect of Shear Resistance Along Vertical Sides

Fig. 4 presents a relationship between the ratio of 3D/2D factors of safety (3D/2D FS) and W/H for the three slope inclinations considered in the parametric study. The two different slope heights of 10 and 100 m were also used but there was little, if any, difference between the factors of safety. For example, the 3D/2D FS ratio versus W/H results at H=10 and 100 m for the 1H:1V slope were the same. For the 3H:1V slope, the 3D/2D FS ratio versus W/H results at H=10 and 100 m were nearly the same with differences in 3D/2D FS ratios not exceeding 0.05. For the 5H:1V slope, the 3D/2D FS ratio versus W/H results at H=10 and 100 m differed by less than 0.06 for W/H values greater than 1.5. At a W/H ratio of 1, the 3D/2D FS ratio difference was 0.19. The slight differences in the 3D/2D FS ratio versus W/H results obtained at H = 10 and 100 m for the three slope inclinations is probably caused by the affects of CLARA 2.31 moving each input cross section so the x-coordinate coincides with the nearest row of column center points and the interpolation between these input cross sections which influences determination of 3D column parameters. In summary, slope heights of 10 and 100 m did not significantly affect the relationship between the ratio of 3D/2D factors of safety and W/H for the slope inclinations considered. This observation is in agreement with the concept of geometric similarity.

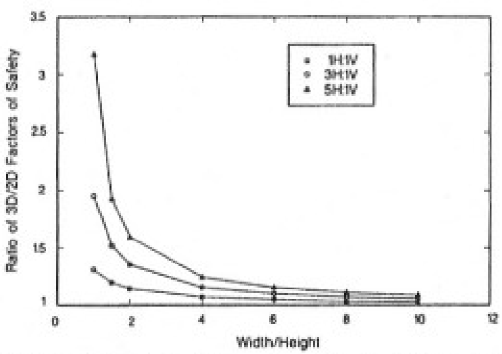

Figure 4. Effect of Shear Resistance along Vertical Sides of Slide Mass

The 3D factor of safety was greater than the 2D factor of safety for all of the W/H combinations used in the parametric study. It can be seen from Fig. 4 that the 3D/2D FS ratio increases with decreasing W/H ratios for a given slope inclination. The area of the vertical, parallel sides of the slide mass are the same for a given slope inclination and height for all width values. As the width decreases, the weight

of the slide mass decreases and the shearing resistance along the parallel sides has a greater effect on the 3D stability. This is evidenced in Fig. 4 because the relationships increase rapidly at values of W/H less than 4. For W/H ratios less than 1.5, 3, and 5, the 3D factor of safety is at least 20 percent greater than the 2D factor of safety for the three slope inclinations. Therefore, the effect of including shearing resistance along the parallel sides of a slide mass increases as the slope width decreases.

Fig. 4 also shows that as the slope inclination decreases, for a given W/H ratio, the 3D/2D FS ratio increases. This increase in 3D/2D FS ratio for a given W/H ratio results from an increase in the area of the vertical sides of the slide mass due to the increase in L with decreasing slope inclination. Therefore, the importance of incorporating end effects in a slope stability analysis increases with decreasing slope inclination. Chen and Chameau (1983) and Leshchinsky et al. (1985) also indicate that the flatter the slope, the greater the difference between 2D and 3D factors of safety. Therefore, in translational failures, which can occur in relatively flat slopes because of the presence of underlying weak material(s), the back-calculated shear strengths may be too high if end effects on the sides of the slide mass are ignored.

Influence of Shear Strength

The results in Fig. 4 are based on a ratio of friction angles for the upper (30°) and lower (8°) materials, ϕ_{up}/ϕ_l, of 3.75. Additional ratios of ϕ_{up}/ϕ_l, e.g., 1, 1.5, 3, and 3.75, were used to investigate the influence of various friction angle ratios on the 3D/2D FS ratio values. To obtain these lower ratios of ϕ_{up}/ϕ_l, the friction angle of the lower material was increased. The friction angle of the upper material remained 30 degrees so the back scarp would remain inclined at 60° and thus simulate an active pressure condition as previously discussed. It was assumed that the value of unit weight of the lower material was 18 kN/m^3 and did not vary with ϕ_l. Figs. 5 through 7 show the results of these analyses for slope inclinations of 1H:1V, 3H:1V, and 5H:1V, respectively. Each relationship shown in Figs. 5 through 7 for a given W/H is the average obtained from the 3D/2D FS ratio versus ϕ_{up}/ϕ_l results obtained at H = 10 and 100 m. It can be seen from Fig. 7 that varying the ratio of ϕ_{up}/ϕ_l was most pronounced for the 5H:1V slope. The effect of varying ϕ_{up}/ϕ_l decreased for increasing W/H. For example, for a 5H:1V slope (Fig. 7) and a value of W/H of 10 and 1, the difference in the 3D/2D FS ratio ranged from 1.6 to 2.1, respectively, for the range of ϕ_{up}/ϕ_l ratios investigated.

Figs. 5 through 7 also show that for a given W/H ratio and back scarp angle, the influence of shear strength between the upper and lower layers increases with decreasing slope inclination. For a W/H of 1.0, back scarp angle of 60°, and a ϕ_{up}/ϕ_l of 3.75, the 3D/2D FS ratio increased from 1.31 to 3.18 for slopes of 1H:1V

(Fig. 5) to 5H:1V (Fig.7), respectively. For flatter slopes at a given W/H and back scarp angle, the L/H increases. Thus, the flatter slope yields a larger value of L and a larger shear stress is mobilized along the base of the sliding surface. In the previous section, it was shown that the influence of incorporating end effects in a slope stability analysis increases with decreasing slope inclination for a given W/H Ratio (see Fig. 4). The results of Figs. 5 through 7 indicate that this influence may become more substantial with larger differences in shear strength between upper and lower layers. Thus, in relatively flat slopes with large differences in in-situ material shear strengths, the back-calculated shear strengths may be too high or unconservative. This is especially true in translational failures that occur in relatively flat slopes where the underlying material(s) may be much weaker than the upper materials.

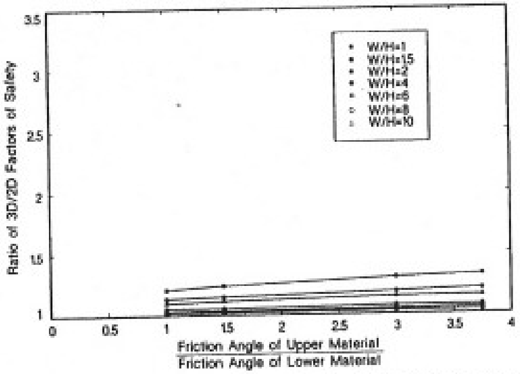

Figure 5. Influence of Shear Strength on Ratio of 3D/2D Factors of Safety for 1H:1V Slope

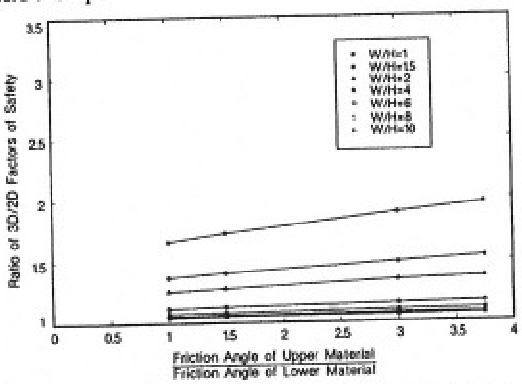

Figure 6. Influence of Shear Strength on Ratio of 3D/2D Factors of Safety for 3H:1V Slope

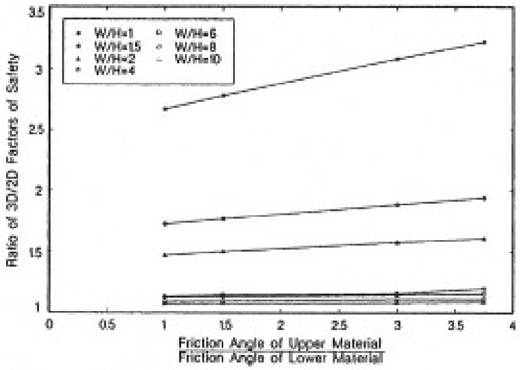

Figure 7. Influence of Shear Strength on Ratio of 3D/2D Factors of Safety for 5H:1V Slope

Figs. 8 and 9 illustrate the influence of ϕ_{up}/ϕ_l on the 2D and the 3D factors of safety, respectively, instead of using a FS ratio. These figures indicate that the effect of varying the friction angle between the upper and lower layers is more significant on the 3D factor of safety than the 2D FS value. The results of Figs. 8 and 9 indicate that the 3D/2D FS ratio differences obtained in Figs. 5 through 7 are due primarily to changes in the 3D factor of safety rather than to changes in the 2D factor of safety. Therefore, it is even more important that material shear strength parameters are adequately defined for a 3D analysis than a 2D analyses.

This parametric study was performed based on the assumption that materials along the vertical sides of the slide mass consist of cohesionless materials, i.e., cohesion, c=0. Previous studies have indicated that the 3D end effects are more pronounced for slopes of cohesive materials (Chen 1981; Lovell 1984; Leshchinsky and Baker 1986; Ugai 1988).

Field Case History

A field case history is presented to illustrate the use of the parametric study results and the importance of conducting a 3D analysis in practice. The 1979 Oceanside Manor landslide occurred in San Diego County, California and is described in detail by Stark and Eid (1998). The landslide occurred along a bluff approximately 20 m high in a residential area. The length of the scarp is approximately 130 m and the slide encompassed approximately 122,000 m^3 of soil. A plan view and representative cross section of the landslide prior to failure are presented by Stark and Eid (1998). The slope is underlain by the Santiago Formation, which is composed of a claystone and a sandstone. The sandstone is fine to medium grained and overlies the gray claystone. The remolded claystone classifies as a clay or silty clay of high plasticity, CH-MH, according to the Unified Soil Classification System. The liquid limit, plasticity index, and clay-size fraction are 89, 45, and 57 percent, respectively (Stark and Eid 1992).

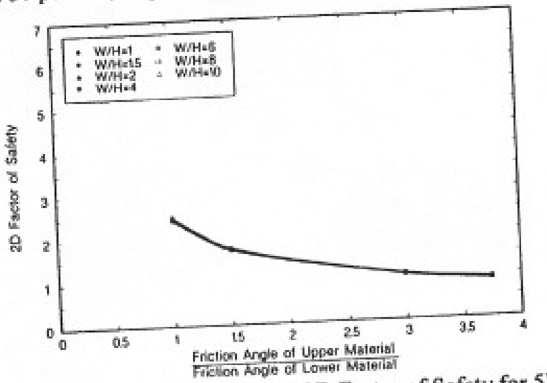

Figure 8. Influence of Shear Strength on 2D Factor of Safety for 5H:1V Slope

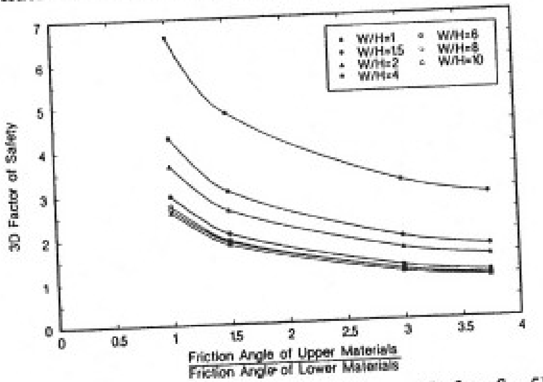

Figure 9. Influence of Shear Strength on 3D Factor of Safety for 5H:1V Slope

Field investigations showed that the claystone is commonly fissured, displaying numerous slickensided surfaces. The site has undergone at least three episodes of landsliding prior to this slide. Therefore, the claystone has undergone substantial shear displacement and has probably reached a residual strength condition along the base of the sliding surface. In addition, the largest portion of the sliding surface in the claystone is approximately horizontal through the Santiago Formation. This indicates that sliding occurred along a weak claystone seam or layer. As a result, Stark and Eid (1998) assumed that residual and fully softened shear strengths were mobilized during failure along the base and the scarp in the Santiago Formation, respectively. The slide surface was located using slope

inclinometers and extensive borings and trenches. The groundwater levels were monitored using piezometers and water levels in borings and trenches shortly after movement started to occur.

Stark and Eid (1998) performed 3D and 2D slope stability analysis. The parallel sides of the sliding mass were assumed to be nearly vertical. In addition, the back scarp was taken to be inclined 60 degrees from the horizontal to simulate an active earth pressure condition. Moist unit weights for the Santiago claystone and the compacted fill were measured to be 19.6 kN/m^3. Based on residual and fully softened shear strengths measured on representative samples of the Santiago claystone using a ring shear test procedure, a residual friction angle of 7.5 degrees and a fully softened friction angle of 25 degrees was used for the claystone in the slope stability analyses. The fully softened friction angle of the claystone along the back scarp was used for calculating the mobilized shear strength of the sliding mass. The cohesion and friction angle of the compacted fill were measured using direct shear tests to be zero and 26 degrees, respectively.

An average 2D factor of safety of 0.92 was reported based on the analysis of 44 different cross sections and a 3D factor of safety of 1.02 was calculated. The 2D and 3D slope stability results were conducted using Janbu's simplified method and the microcomputer program CLARA 2.31. The factors of safety values are uncorrected for the effect of the interslice or intercolumn force distribution.

This case history is used to demonstrate the use of the results of the parametric study (Figs. 5 through 7). The slope had an average slope inclination of 3.5H:1V prior to failure. The W/H ratio is 130 m/20 m or 6.5. The ϕ_{up}/ϕ_l ratio (25 degrees divided by 7.5 degrees) is 3.3. Using Fig. 6, a W/H of 6.5, and $\phi_{up}/\phi_l = 3.3$, a 3D/2D ratio of 1.09 is obtained for a slope of 3H:1V. Similarly, from Fig. 7, a 3D/2D FS ratio of 1.14 is obtained for a slope of 5H:1V. For the landslide slope inclination of 3.5H:1V, a 3D/2D FS ratio of 1.1 can be interpolated from Figs. 6 and 7. Based on the average 2D factor of safety of 0.92 from 44 different cross-sections reported by Stark and Eid (1998), the 3D factor of safety can be estimated to be 1.01 using the 3D/2D FS ratio of 1.1. This estimated 3D factor of safety is in agreement with the 3D factor of safety value of 1.02 calculated by Stark and Eid (1998).

It should be noted that the slope inclinations in Figs. 4 through 9 represent an average inclination across the landslide. Additionally, the 2D value represented by the 3D/2D FS ratios in Figs. 4 through 8 is an average 2D factor of safety value across the landslide in the direction of movement. The ratio between the 3D factor of safety and the minimum 2D factor of safety may be slightly larger in practice due to the simplified model. For the Oceanside Manor case history the ratio between the 3D factor of safety and minimum 2D factor of safety is 1.6 (Stark and Eid 1998).

In summary, Figs. 5 through 7 can be used to determine the importance or necessity of performing a 3D slope stability analysis for a translational failure mode in practice. However, these figures should not be used as a substitute for performing an actual 3D slope stability analysis with site specific geometry, pore-water pressure condition, and material properties.

Conclusions

Commercially available 3D slope stability software do not consider the shear resistance along the two vertical sides of the slide mass that parallel the direction of movement in calculating the 3D factor of safety. A method for incorporating the shear resistance along the two sides of a slide mass is presented and consists of placing a horizontal and vertical external force equivalent to the shear resistance due to the at-rest earth pressure acting at the centroid of the sides parallel to the direction of movement of the slide mass. A parametric study was conducted to investigate the importance of incorporating 3D end effects for various slope geometries and shear strengths. The following conclusions are based on the 2D and 3D slope stability analyses performed in the parametric study:

(1) For a given slope inclination, the ratio of 3D/2D factors of safety increases with decreasing W/H ratios. As the width decreases, the weight of the slide mass decreases and the shearing resistance along the parallel sides has a greater effect on the 3D stability. Therefore, the effect of including the shear resistance along the parallel sides of a slide mass can be significant for slopes that have a W/H ratio of less than 4.

(2) As the slope inclination decreases for a given W/H ratio, the 3D/2D factors of safety ratio increases. This increase in the factor of safety ratio results from an increase in the area of the parallel sides of the slide mass caused by the increase in slope length with decreasing slope inclination. Therefore, the influence of incorporating end effects in a slope stability analysis increases with decreasing slope inclination. In translational failures involving slope inclinations less than 3H:1V, the back-calculated shear strengths may be too high if 3D end effects on the sides of the slide mass are ignored. For a given W/H ratio and back scarp angle, the impact of the shear strength in the upper and lower layers increases with decreasing slope inclination.

(3) The difference in shear strength between the upper and lower layers has a larger effect on the 3D factor of safety than on the 2D factor of safety. This effect of the shear strength difference increases with decreasing W/H ratios. Therefore, it is critical that material shear strengths be adequately defined for a 3D analysis.

(4) Figs. 5 through 7 presented herein can be used to determine the importance of performing a 3D slope stability analysis for a translational failure mode. The use of Figs. 5 through 7 is illustrated using a field case history. However, these figures should not be used as a substitute for performing an actual 3D slope stability analysis with site specific geometry, pore-water pressure condition, and material properties.

Commercially available 3-D slope stability software has inherent limitations that affect the calculated factor of safety for a translational failure mode (Stark and Eid 1998). These limitations include ignoring the shear resistance along the sides parallel to the direction of movement of the sliding mass, modeling a nonlinear failure envelope with a linear failure envelope, and using a 3-D slope stability method that ignores some of the internal shear forces. Commercially available 3D numerical modeling software that utilize numerical methods such as the finite element method provide a powerful alternative to the limit equilibrium approach for investigating slope stability problems because numerical methods may alleviate these limitations. The use of these numerical methods is the subject of subsequent research.

Acknowledgments

The first author acknowledges the support provided by the State of Illinois Minority Graduate Incentive Program. This study was performed as a part of National Science Foundation Grant CMS-98-02615. The support of this agency is gratefully acknowledged. The second author also acknowledges the support provided by a University Scholar Award. The authors acknowledge the support provided by Dr. Oldrich Hungr of O. Hungr Geotechnical Research Inc. The contents and views in this paper are the authors' and do not necessarily reflect those of any of the contributors or represented organizations.

References

Beene, R. R. W. (1967), "Waco Dam Slide," *Journal of Soil Mechanics and Foundations Division, ASCE*, 93(4): 35-44.
Byrne, R .J., Kendall, J., and Brown, S. (1992), "Cause and Mechanism of Failure, Kettleman Hills Landfill B-19, Unit IA," *Proceedings of Stability and Performance of Slopes and Embankments-II*, ASCE, Vol. 2, pp. 1188-1215.
Chen, R.H. (1981), *Three-Dimensional Slope Stability Analysis*, Report JHRP-81-17, Purdue University, West Lafayette, IN, USA.
Chen, R.H. and Chameau, J.-L. (1983), "Three-Dimensional Limit Equilibrium Analysis of Slopes," *Geotechnique*, 32(1): 31-40.
Duncan, J.M. (1992), "State-of-the-Art: Static Stability and Deformation Analysis," *Proceedings of Stability and Performance of Slopes and Embankments-II*, ASCE, Vol. 1, pp. 222-266.

Ehlig, P. L. (1992), "Evolution, Mechanics and Mitigation of the Portuguese Bend Landslide, Palos Verdes Peninsula, California," *Engineering Geology Practice in Southern California*, B. W. Pipkin and R. J. Proctor, eds., Star Publishing Co., Belmont, Calif., pp. 531-553.

Hungr, O. (1988), *User's Manual CLARA: Slope Stability Analysis in Two or Three Dimensions for IBM Compatible Microcomputers*, O. Hungr Geotechnical Research, Inc., West Vancouver, B.C.

Hungr, O., Salgado, F.M., and Byrne, P.M. (1989). "Evaluation of a three-dimensional method of slope stability analysis," *Canadian Geotechnical Journal*, 26: 679-686.

Janbu, N. (1954), *Stability Analysis of Slopes with Dimensionless Parameters*, Harvard University, Soil Mechanics Series, No. 46. Harvard University, Cambridge, Mass.

Jasper, J. L., and Peters, N. (1979), "Foundation Performance of Gardiner Dam," *Canadian Geotechnical Journal*, 16: 758-788.

Krahn, J., Johnson, R. F., Fredlund, D. G., and Clifton, A. W. (1979), "A Highway Cut Failure in Cretaceous Sediments at Maymont, Saskatchewan," *Canadian Geotechnical Journal*, 16:703-715.

Leshchinsky, D., Baker, R. and Silver, M. L. (1985), "Three Dimensional Analysis of Slope Stability," *International Journal for Numerical and Analytical Methods in Geomechanics*, 9(2): 199-223.

Leshchinsky, D. and Baker, R. (1986), "Three-Dimensional Slope Stability: End Effects," *Soils and Foundations*, 26(4): 98-110.

Lovell, C.W. (1984), "Three Dimensional Analysis of Landslides," *Proceedings of the 4th International Symposium on Landslides*, Toronto, pp. 451-455.

Seed, R.B., Mitchell, J.K. and Seed, H.B. (1990), "Kettleman Hills Waste Landfill Slope Failure. II: Stability Analysis," *Journal of Geotechnical Engineering*, ASCE, 116(4): 669-689.

Stark, T.D. and Eid, H. T. (1992), "Comparison of Field and Laboratory Residual Shear Strengths," *Proceedings of Stability and Performance of Slopes and Embankments-II*, ASCE, Vol. 1, pp. 876-889.

Stark, T.D. and Eid, H. T. (1998), "Performance of Three-Dimensional Slope Stability Methods in Practice," *Journal of Geotechnical and Geoenvironmental Engineering*, ASCE, 124(11): 1049-1060.

Stark, T.D. and Poeppel, A.R. (1994), "Landfill Liner Interface Strengths from Torsional Ring Shear Tests," *Journal of Geotechnical Engineering*, ASCE, 120(3): 597-615.

Ugai, K. (1988), "Three-Dimensional Slope Stability Analysis by Slice Methods," *Proceedings of the 6th International Conference on Numerical Methods in Geomechanics*, Innsbruck, pp. 1369-1374.

Wright, S. G., and Duncan, J. M. (1972), "Analyses of Waco Dam Slide," *Journal of Soil Mechanics and Foundations Division*, ASCE, 98(9): 869-877.

A Numerical Technique for Two-Dimensional Slope Stability Problems

Mohsen Beikae [1]

Abstract

All limit equilibrium methods of slope stability analysis 1) calculate a factor of safety which is assumed to be the same at all points along the potential slip surface, 2) use only force and moment equilibrium and employ varying assumptions to make the problem statically determinate, 3) assume that the potential sliding mass is a rigid body, 4) need a direction of movement of a potential sliding mass for three-dimensional cases, and 5) calculate a yield acceleration to be used in the Newmark method. To facilitate the slope stability analysis and to avoid some of the above limitations, a numerical technique has been developed and a computer program written to carry out the analysis technique. A single analysis determines local factors of safety and a pattern of induced deformations of a potential sliding mass due to gravity, hydrostatic forces, and base motions. Results of analyses for two example slopes are given to demonstrate the comparison between this technique and the conventional methods.

Introduction

A commonly accepted practice in slope design is to use limit equilibrium methods of slope stability analysis. As noted by Duncan and Wright (1980), all limit equilibrium methods have four characteristics in common: 1) a factor of safety is placed on shear strength parameters, 2) the strength parameters are independent of stress-strain behavior, 3) some or all of the equations of equilibrium are used to determine the factor of safety, and 4) forces involved in equilibrium methods are statically indeterminate. Two other common characteristics, which may be added to the above list, are: 1) the potential sliding mass is assumed to be a rigid body and 2) the direction of least resistance to sliding for a three-dimensional problem is not in general obvious, therefore, a critical direction is assumed.

The limit equilibrium methods calculate a factor of safety which, by definition, is assumed to be the same at all points along the potential slip surface. This is reasonable only at failure, when all the slices are on the verge of failure; that

[1]Engineer, Metropolitan Water District of Southern California, 700 N. Alameda Street, Los Angeles, California 90012